CONSIDERATION OF NEAR-FAULT GROUND MOTION EFFECTS IN SEISMIC DESIGN

Babak ALAVI[1] And Helmut KRAWINKLER[2]

SUMMARY

This paper summarizes the results of a study that is intended to evaluate and quantify salient response attributes of near-fault ground motions. Recordings suggest that near-fault ground motions are characterized by a large high-energy pulse. It is shown that the response of structures to near-fault and pulse-type ground motions has similarities that can be used to represent near-fault records by simple pulses. The parameters of the equivalent pulses are related to magnitude and distance using regression on a data set derived from available near-fault records. Equivalent pulses are used to derive design spectra that can be used to determine the base shear strength of frame structures required to limit the maximum story ductility to a predefined target value. Recommendations are made for story shear force patterns that can improve the distribution of ductility demands over the height of the structure.

INTRODUCTION

Near-fault ground motions, which have caused much of the damage in recent major earthquakes (Northridge 1994, Kobe 1995), are characterized by a short-duration impulsive motion that exposes the structure to high input energy at the beginning of the record. This pulse-type motion is particularly prevalent in the "forward" direction, where the fault rupture propagates towards a site at a velocity close to the shear wave velocity. The radiation pattern of the shear dislocation of the fault causes the pulse to be mostly oriented perpendicular to the fault, causing the fault-normal component of the motion to be more severe than the fault-parallel component [Somerville, 1998]. The need exists to incorporate this special effect in the design process for structures located in the near-fault region. The near-source factors incorporated in recent codes cannot solve the problem consistently, because design procedures should pay attention to the special frequency characteristics of near-fault ground motions. Moreover, the emerging concepts of performance-based design require a quantitative understanding of response to different types of ground motion at different performance levels, ranging from nearly elastic to highly inelastic behavior.

The study summarized in this paper is concerned with the elastic and inelastic response of SDOF systems and MDOF frame structures subjected to near-fault ground motions. The global objective of the study is to acquire quantitative knowledge on near-fault ground motion effects and to develop design guidelines that provide more consistent protection for structures located in near-fault regions. What has been learned from this study is that the near-fault problem is big, indeed, and that much more work is needed before a comprehensive understanding of all important aspects of the problem will be accomplished. This paper merely addresses a few fundamental issues that were investigated in order to form a foundation on which to base future research and development of design guidelines.

[1] *Research Assistant, Dept. of Civil and Environmental Engineering, Stanford Univ., Stanford, CA 94305-4020*
[2] *Professor, Dept. of Civil and Environmental Engineering, Stanford Univ., Stanford, e-mail: hk@ce.stanford.edu*

NEAR-FAULT GROUND MOTIONS AND DUCTILITY DEMANDS FOR FRAME STRUCTURES

Sets of recorded and simulated near-fault ground motions assembled by Somerville [Somerville, 1998] are utilized in this study. Velocity spectra of a typical near-fault ground motion with forward directivity are shown in Fig. 1. The graph includes spectra for the fault-normal and associated fault-parallel components, and for the two 45° rotated (w.r.t. fault-normal) components of the record. The severity of the fault-normal component compared to the fault-parallel component is evident. When these two components are rotated by 45°, the difference in the spectra becomes smaller, but one of the two rotated components still will impose demands close to those associated with the fault-normal direction. This observation is consistent for all the near-fault records investigated in this study. Thus, for a 3-D structure composed of frames in two perpendicular directions, frames in one of these two directions will always get exposed to a ground motion of an intensity close to that of the fault-normal component. This justifies the use of the fault-normal component as the main focus of this study.

Another important observation from the spectra is the existence of a clear peak in the fault-normal velocity spectrum. Such a peak is discernible in all near-fault records, with the caveat that some of the records used in this study have more than one clear velocity peak. As will be discussed later, identifying the predominant peak is the key to estimating the pulse period of a near-fault record.

Figure 2 compares the velocity spectra of several near-fault ground motions recorded on soil type S_D (see Table 1) together with the mean spectrum of 15 reference records (15-D*). These 15 records have been scaled to match the 97 UBC design spectrum for the same type of soil ignoring near-fault effects. This figure illustrates the large diversity of near-fault ground motions and the very high demands that should be expected when a structure is subjected to near-fault excitations.

Table 1. Near-Fault Records Used in Fig. 2

Designation	Earthquake	Station	Magnitude	Distance
LP89lgpc	Loma Prieta, 1989	Los Gatos	7.0	3.5
LP89lex	Loma Prieta, 1989	Lexington	7.0	6.3
EZ92erzi	Erzincan, 1992	Erzincan	6.7	2.0
LN92lucr	Landers, 1992	Lucerne	7.3	1.1
NR94rrs	Nothridge, 1994	Rinaldi	6.7	7.5
NR94sylm	Nothridge, 1994	Olive View	6.7	6.4
KB95kobj	Kobe, 1995	JMA	6.9	3.4
KB95tato	Kobe, 1995	Takatori	6.9	4.3

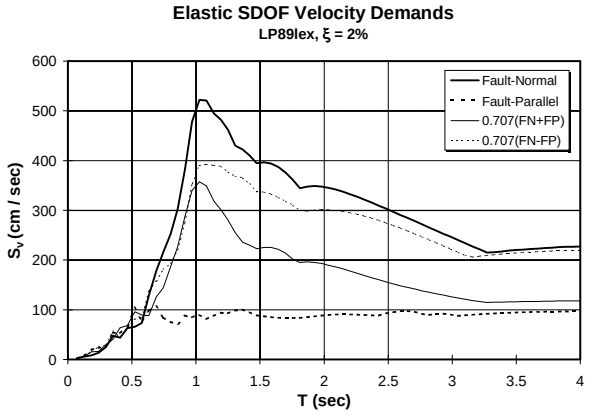

Figure 1. Velocity Spectra of a Near-Fault Record (Fault-Normal, Fault-Parallel, and 45° Comp.)

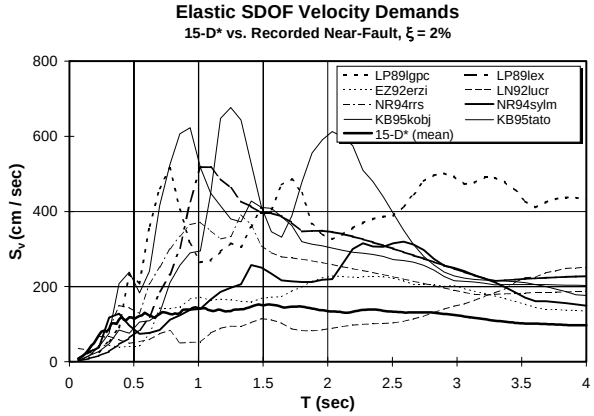

Figure 2. Velocity Response Spectra of Near-Fault and Reference Ground Motions

A 20-story, single-bay generic frame is used to evaluate MDOF seismic demands. The fundamental period and base shear strength of this frame are varied. The base shear strength is defined by the base shear coefficient $\gamma = V_y/W$, where V_y is the base shear strength and W is the seismically effective weight of the structure. The story stiffnesses and shear strengths are determined from a lateral load pattern that corresponds to the story shear forces resulting from the SRSS combination of modal response for a constant velocity response spectrum. This load pattern, which will be referred to as the SRSS pattern, is in line with the provisions of current seismic codes. Therefore, the generic frame used in this study can be viewed as a representative of regular frame structures designed to recent code requirements.

The MDOF model is subjected to the same records as used in Fig. 2 to illustrate how code-designed structures may behave in near-fault regions. Figure 3 shows maximum story ductility ratios for a frame with a fundamental period of 2.0 sec. at two different base shear strength levels, (a) $\gamma = 0.4$ and (b) $\gamma = 0.15$. The period of 2.0 sec. is selected because it is larger than the period of the equivalent pulse contained in most of the

records. This figure indicates how the distribution of story ductility over the height of a long-period structure is affected by strength when subjected to near-fault ground motions. When the structure is relatively strong (γ = 0.4) and the ductility demands are low, the largest demands occur in the upper portion of the structure. However, as the strength of the structure is reduced, the ductility demand in the upper portion stabilizes (at a value around 3 to 5) and the story with the largest ductility demand migrates to the bottom. At a base shear coefficient of γ = 0.15, the largest demand occurs in the bottom stories for all cases. This type of behavior is found to be very consistent for long period structures subjected to near-fault ground motions. Long period implies that the fundamental period of the structure, T, is clearly larger than the period of the equivalent pulse, T_p. The migration of maximum demands is not observed for structures with $T/T_p < 1.0$. This observation points out a design dilemma for long period structures, because improved protection against early yielding necessitates a relative increase in story shear strength in the upper portion of the structure, whereas improved protection against very severe events necessitates a relative increase in strength in the bottom stories.

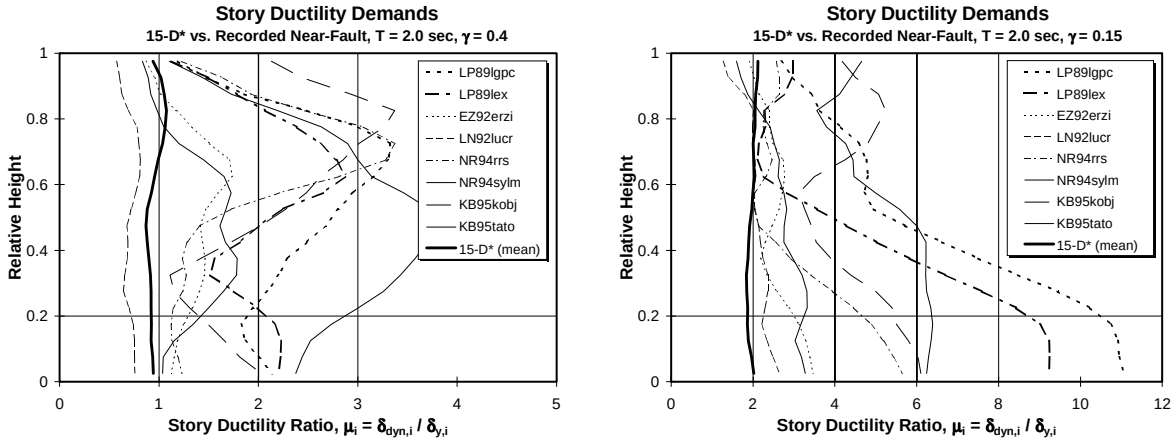

(a) γ = 0.40 (b) γ = 0.15

Figure 3. Story Ductility Demands for Several Near-Fault Records, T = 2.0 sec.

Figure 3 also carries another important message. The mean story ductility demands for the reference record set 15-D* are also superimposed on each graph. It can be seen that the demands for the near-fault records are much higher than those for the records scaled to the 1997 UBC design ground motion spectrum ignoring near-fault effects.

RESPONSE TO SIMPLE PULSES

In order to develop a systematic procedure for assessing near-fault effects, it is useful to try to relate near-fault records to a small number of simple input pulses that can be fully defined by a few parameters. Pulses of various shapes were investigated for this purpose [Alavi and Krawinkler, 1998]. Figure 4 presents the acceleration, velocity and displacement time histories of one of the input pulses studied (designated as P2), which turns out to be capable of resembling many of the near-fault records investigated. This pulse is fully defined by two parameters, i.e., the pulse period (T_p), which is defined as the duration of a complete velocity cycle, and the maximum ground acceleration ($a_{g,max}$) or velocity ($v_{g,max} = a_{g,max}T_p/4$).

Figure 5 shows the acceleration, velocity and displacement spectra of pulse P2, with the spectral values normalized by their corresponding peak time history quantity. The velocity response spectrum shows a peak at $T/T_p = 1.0$ indicating that the peak spectral velocity for pulse-type (and near-fault) ground motions occurs at a period equal to the pulse period T_p.

If the MDOF model is subjected to pulse P2, the distribution of story ductility demands over the height of the structure is as shown in Fig. 6. In this figure the ductility demands are presented for different base shear strengths. For pulse inputs, the strength coefficient η is defined as $\eta = V_y/(m.a_{g,max})$, where m is the seismically effective mass of the structure. It should be noted that a low η value can represent either a weak structure (low V_y) or a severe ground motion (high $a_{g,max}$). The ductility patterns in Fig. 6(a), for $T/T_p = 2.0$, are similar to those observed in Fig. 3 for recorded ground motions, i.e., the demands are highest in the upper portion for relatively strong structures and migrate towards the bottom as the strength of the structure decreases. This phenomenon of migration of maximum ductility demands towards the bottom is not observed for the structure

with $T/T_p = 1.0$ (Fig. 6(b)), simply because the maximum demands for strong structures already are highest near the bottom. This behavior pattern is consistent for near-fault ground motions and pulse responses, indicating the need to distinguish between structures with $T/T_p > 1.0$ and $T/T_p \leq 1.0$. The response of the former is greatly affected by the effects of a wave traveling up the structure, which causes high shear demands in the upper portion for cases of close to elastic behavior.

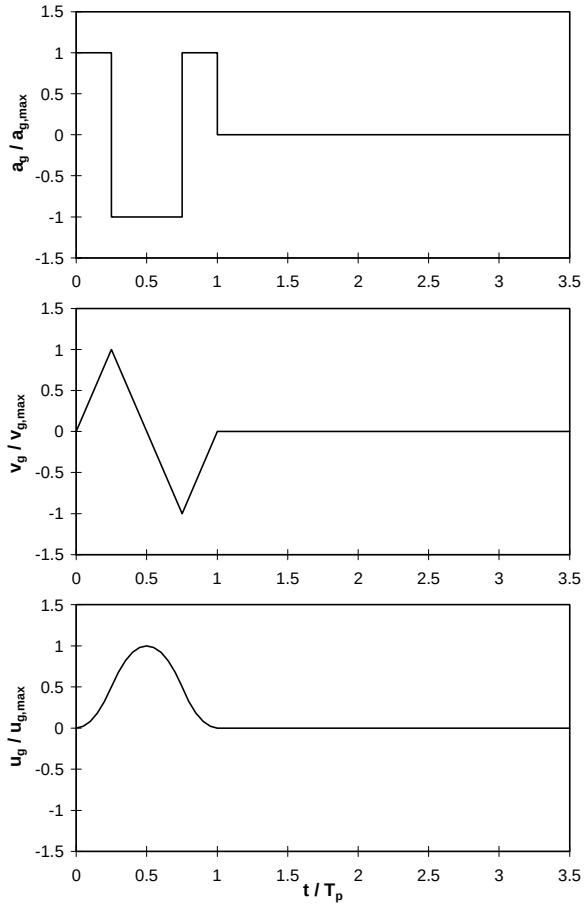

Figure 4. Acceleration, Velocity and Displacement Time Histories of Pulse P2

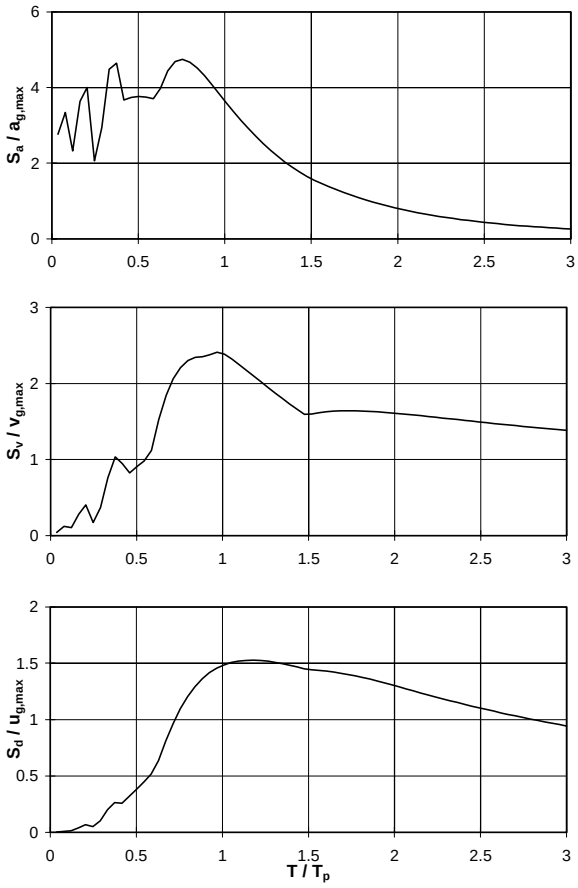

Figure 5. Acceleration, Velocity and Displacement Spectra of Pulse P2

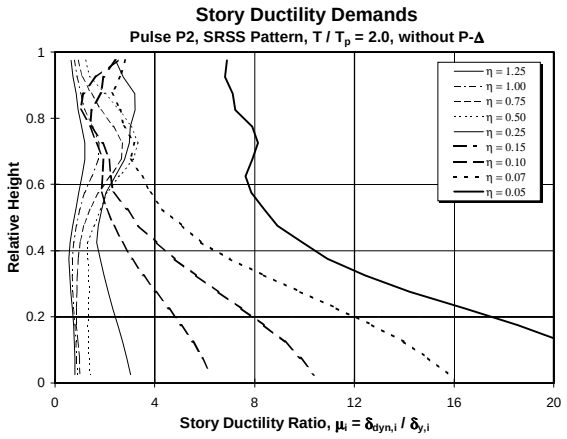

(a) $T/T_p = 2.0$

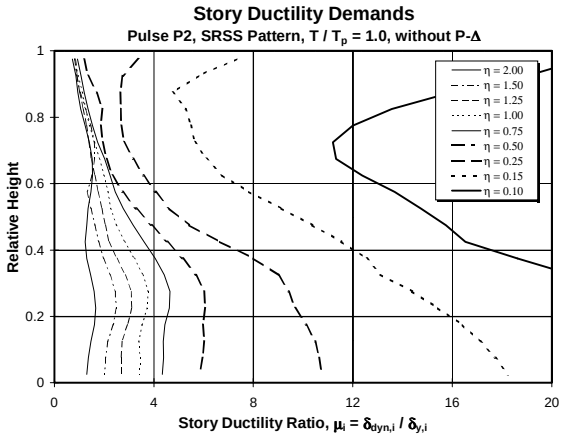

(b) $T/T_p = 1.0$

Figure 6. Story Ductility Demands for Pulse P2, Various Base Shear Strength Values η

Using information of the type presented in Fig. 6, base shear strength demand spectra for targeted maximum ductility of MDOF systems can be developed. Fundamental to this development are $\eta - \mu_{max}$ curves of the type illustrated in Fig. 7. They represent peak ductility values taken from the plots presented in Fig. 6. Vertical cuts through the graph of Fig. 7 provide values for the constant ductility strength demand spectra. Figure 8 shows such spectra for pulse P2. These spectra define the base shear strength required to limit the maximum story ductility demand anywhere in the structure to specified target values. Inherent in these spectra is the assumption of a story shear strength distribution over the height according to the SRSS load pattern defined previously.

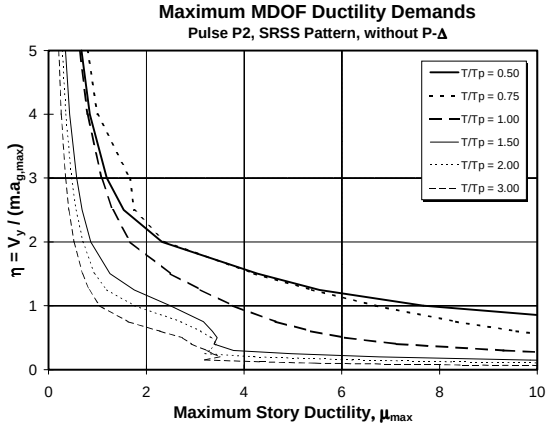

Figure 7. MDOF Base Shear Strength vs. Max. Story Ductility Demand for Various T/T_p, Pulse P2

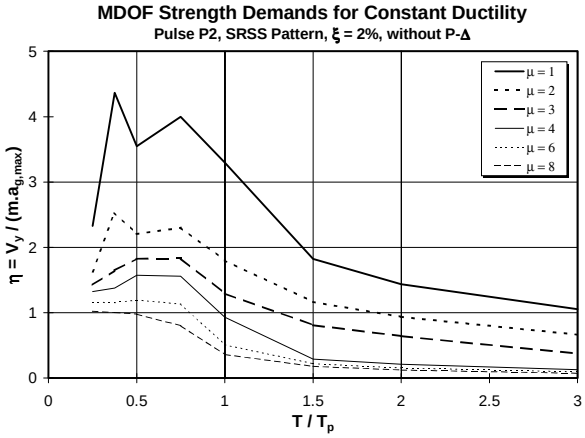

Figure 8. MDOF Base Shear Strength Demands for Target Maximum Story Ductility Ratios, Pulse P2

Graphs of the type shown in Fig. 8 are very useful for near-fault design because they provide the required strength for various targeted ductility levels, provided that the period and severity of the pulse contained in the near-fault record are known. Thus, the process hinges upon establishing equivalent pulses for near-fault ground motions, which are capable of replicating the most important response characteristics of near-fault records with sufficient accuracy. In particular, if pulse P2 is to represent a near-fault ground motion, the pulse period (T_p) and severity (either $a_{g,max}$ or $v_{g,max}$) for that ground motion will need to be determined.

The authors have established equivalent pulses for a set of recorded and simulated near-fault ground motions [Krawinkler and Alavi, 1998]. The pulse period is identified from the location of a global and clear peak in the velocity spectrum. To determine the pulse severity, an elaborate method is employed that is based on minimizing the differences between the maximum story ductility demand from the near-fault record and the corresponding demand obtained from the equivalent pulse for a certain range of ductility. An important outcome of this effort was that in almost all cases the equivalent pulse velocity lies within 20% of the peak ground velocity of the record. Thus, the peak ground velocity appears to be a simple and stable measure of the pulse severity. As a general conclusion, equivalent pulses prove to be capable of representing near-fault ground motions within some limitations, and the accuracy of such a representation is not equally good in all cases.

MAGNITUDE AND DISTANCE DEPENDENCE OF BASE SHEAR STRENGTH DEMANDS

Given the period and severity of the equivalent pulses that represent near-fault ground motions, regression analysis can be employed to evaluate the magnitude and distance dependence of these parameters. Only relatively small sets of recorded near-fault records are available for this purpose, and the results of such a regression analysis need to be interpreted with caution. Nevertheless, this exercise was performed with the sets of records available to the authors [Somerville, 1998] in order to provide preliminary information on expected pulse parameters. Using a formulation proposed by Somerville [Somerville, 1998], in which it is assumed that the pulse period (T_p) is a function of moment magnitude (M_w), and the pulse severity measure ($v_{g,max}$) is a function of M_w and the shortest distance from the site to the fault (R), and using the results of the equivalent pulse evaluation, the following regression equations are obtained for the pulse parameters:

$$\log_{10} T_p = -1.76 + 0.31\, M_w \qquad (1)$$

$$\log_{10} v_{g,max} = -2.22 + 0.69\, M_w - 0.58 \log_{10} R \qquad (2)$$

Figures 9 and 10 illustrate these equations together with the data points to which the line in Eq. 1 and the surface in Eq. 2 are fitted. It should be noted that in Fig. 9 some of the circles correspond to more than one data point. Since the records used in the regression analysis come from different events with different faulting mechanisms and geology, a large scatter is observed, especially for T_p. It will be shown later that a limited variation in T_p does not have a very large effect on the base shear strength demands obtained from the equivalent pulse approach.

Given the earthquake event parameters R and M_w, the pulse parameters T_p and $a_{g,max}$ (= $4v_{g,max}/T_p$) can be estimated from Eqs. 1 and 2, and the $\eta - T/T_p$ curves presented in Fig. 8 can be converted into γ-T curves [$\gamma = (a_{g,max}/g)\eta$]. The γ-T curves represent MDOF base shear strength demand spectra for specified target ductilities. Examples of such base shear strength demand spectra are presented in Figs. 11 and 12 for various combinations of magnitude and distance. Superimposed on each graph is the corresponding 97 UBC soil type S_D spectrum with and without the code-specified near-fault factor. The UBC spectra are scaled down by a factor of 4, which accounts for a strength reduction factor of 8 and an overstrength factor of 2. The figures, which represent preliminary results, indicate that the strength demands for reasonable target ductilities depend strongly on the period range of interest and may be much larger than those provided by present code designs. The predictions for a magnitude 7.5 event and small distances (Fig. 12) are disconcerting.

The large scatter of the data shown in Fig. 9 provides little confidence in estimating T_p. It turns out that the strength demand spectra are not very sensitive to a limited variation in the pulse period. This is illustrated in Fig. 13, which shows the strength demand spectra, for a target ductility of 2.0, M_w = 7.0, and R = 3 km. In this figure T_p is varied around the value obtained from Eq. 1 for M_w = 7.0 (2.6 sec.). As can be seen, the equivalent pulse strength demands are not severely affected by the variation in T_p, especially for long-period structures.

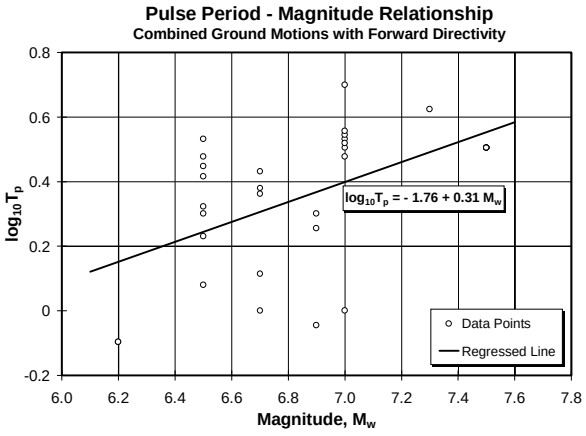

Figure 9. Dependence of Equivalent Pulse Period on Magnitude

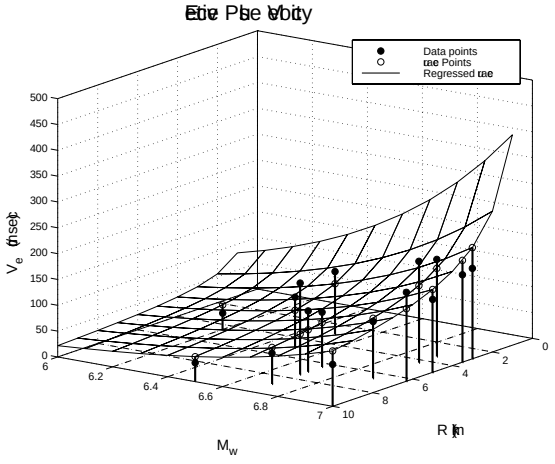

Figure 10. Dependence of Equivalent Pulse Velocity on Magnitude and Distance

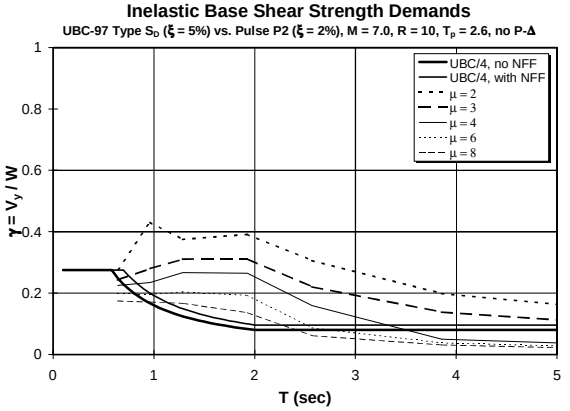

(a) R = 10 km

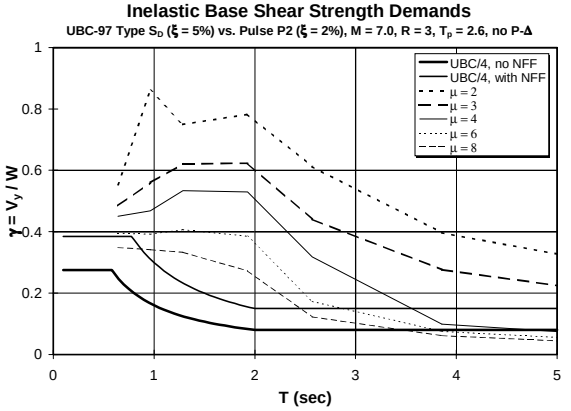

(b) R = 3 km

Figure 11. Base Shear Strength Demands for Equivalent Pulse P2 and a Magnitude 7 Earthquake

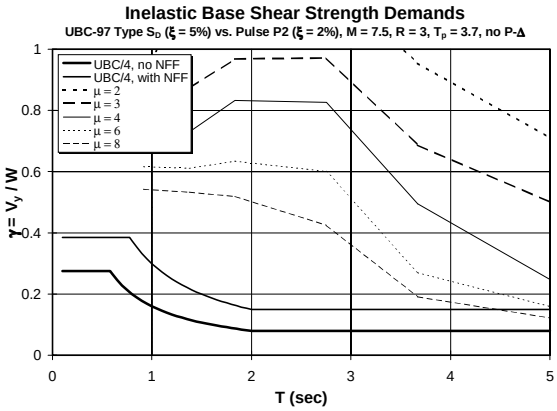

Figure 12. Base Shear Strength Demands for Equiv. Pulse P2 and a Magnitude 7.5 Earthquake, R = 3 km

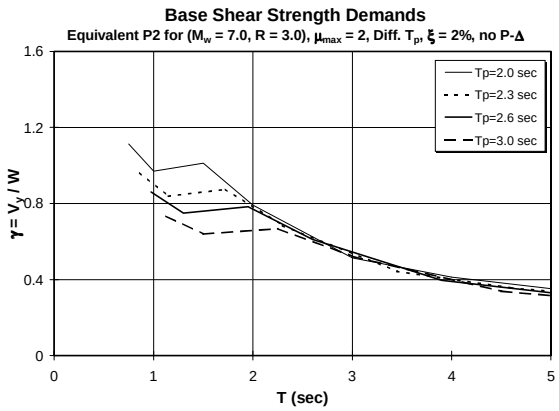

Figure 13. Sensitivity of Base Shear Strength Demands to T_p, M_w = 7.0, R = 3 km, μ = 2

EFFECT OF STORY SHEAR STRENGTH DISTRIBUTION OVER HEIGHT

In the results presented so far a standard SRSS story shear strength distribution over the height has been assigned to the generic structure. Figures 3 and 6 demonstrate that this strength pattern leads to large variations of ductility demands over the height. Therefore, the standard SRSS pattern may not be the most suitable one for protection against near-fault effects. Ideally, story shear strength should be assigned in a manner that causes constant story ductility over the height of the structure. In a pilot study it was found that shear strength patterns for constant story ductility are strongly dependent on the target ductility ratio, particularly for near-fault ground motions and structures with $T/T_p > 1.0$. This is illustrated in Fig. 14 for pulse P2 and different target ductility ratios. The SRSS pattern is also superimposed in this figure. The figure shows that for long period structures ($T/T_p = 2.0$) and close to elastic behavior (μ = 1 and 2) relatively high strength is required around $2/3^{rd}$ up the structure to control ductility demands in the top portion, whereas for a target ductility of 3 or larger the bottom portion needs to be very strong and the required strength decreases rapidly with height. Thus, vastly different strength patterns are obtained as a function of the target ductility. Moreover, the patterns are very different for structures with $T/Tp \leq 1.0$. The conclusion is that no single story shear strength pattern will provide consistent protection at different performance levels and for structures with different periods.

Presuming that it is of primary concern to prevent excessive ductilities in very severe events, it appears to be appropriate to strengthen the bottom of the structure compared to the standard SRSS story strength pattern. Such a strengthening technique was investigated, using the story strength pattern shown in Fig. 15. In this option, the lower 30% of the structure is strengthened compared to the SRSS design with a linear strength increase leading to 40% extra strength at the base. The story ductility demands for structures with $T/T_p = 2.0$ and $T/T_p = 1.0$, designed using the new shear strength pattern, are shown in Fig. 16. The graphs can be compared directly with Fig. 6 to evaluate the benefits achieved by adding the extra strength, which is obviously associated with extra cost.

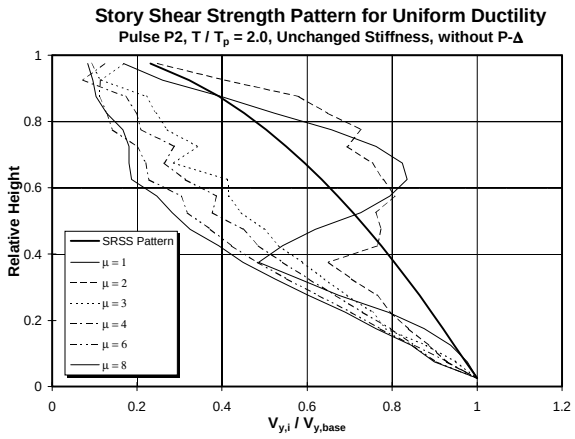

Figure 14. Story Shear Strength Patterns Leading to Constant Ductility Over Height, Pulse P2

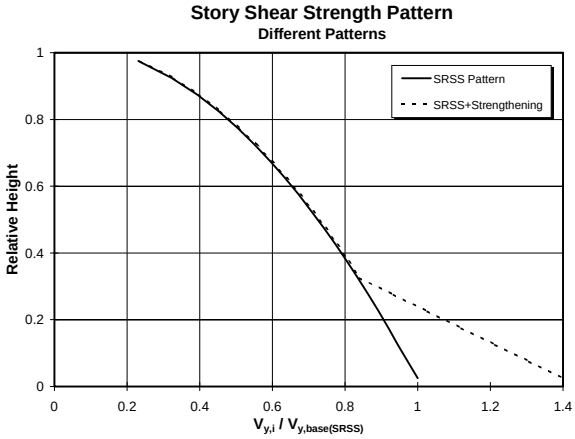

Figure 15. SRSS and Modified Story Shear Strength Patterns

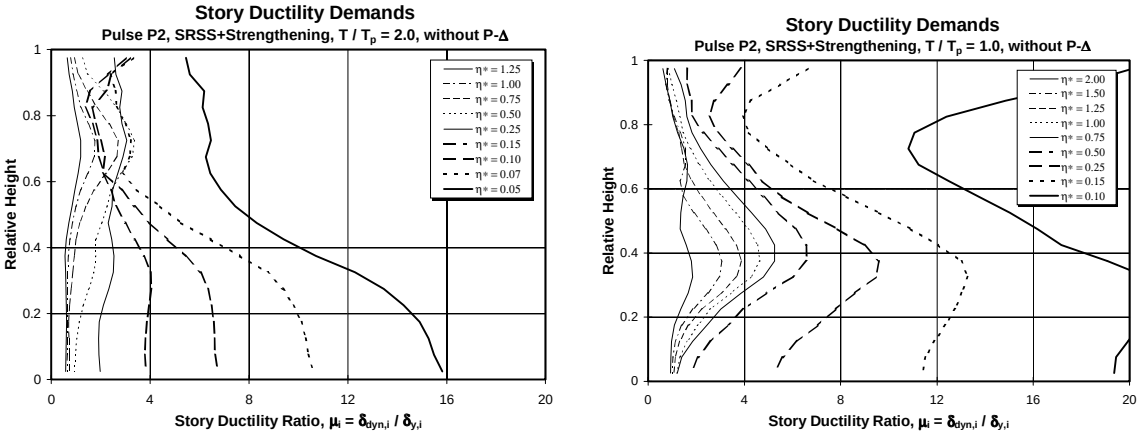

(a) $T/T_p = 2.0$ (b) $T/T_p = 1.0$

Figure 16. Story Ductility Demands for Strengthened Structures, Pulse P2

The benefits in reducing the maximum ductility demands are evident for the structure with $T/T_p = 2.0$. The demands become more uniform over the lower portion and the maximum demand decreases by a factor larger than the strength increase factor of 1.4 in most cases. The benefits for the structure with $T/T_p = 1.0$ are not as evident. For this structure the ductility distribution without strengthening (Fig. 6(b)) is already rather uniform over the lower portion, and the effect of strengthening is to reduce the demand at the very bottom. But the reduction in the maximum ductility demand is minor because the effect of strengthening diminishes at the level at which no strengthening is provided. More work needs to be done to evaluate strengthening techniques.

CONCLUSIONS

- The fault-normal component of the near-fault ground motions with forward directivity is severe and shows pulse-type characteristics. At least one of the 45° components is almost as severe as the fault-normal one.
- Under near-fault excitations, code-prescribed story shear strength patterns lead to a highly non-uniform distribution of ductility demands over the height. In strong long-period structures, early yielding of upper stories occurs, while in weak structures high ductilities occur in bottom stories.
- Equivalent pulses are capable of representing the salient response features of near-fault ground motion.
- Relationships between equivalent pulse parameters and earthquake magnitude and distance, together with pulse strength demand spectra, can be used to evaluate the base shear strength required to limit story ductility ratios to specific target values.
- No single strengthening pattern will improve seismic performance in all cases. Strengthening of bottom stories provides more uniform ductilities and controls excessive demands for long period structures.

ACKNOWLEDGEMENTS

The research summarized here was supported by a grant from the CUREe/Kajima research program and by the California Department of Conservation as a SMIP 1997 Data Interpretation Project. This support is greatly appreciated.

REFERENCES

Alavi, B. and Krawinkler, H. (1998), "Structural Design Implications of Near-Field Ground Motion - Year 2 Research Report", Kajima-CUREe Research Report 1998.11, Kajima Corporation, Tokyo, Japan.

Krawinkler, H. and Alavi, B. (1998), "Development of Improved Design Procedures for Near Fault Ground Motions", *SMIP98 Seminar on Utilization of Strong-Motion Data*, Oakland, CA.

Somerville, P.G. (1998), "Development of an Improved Ground Motion Representation for Near Fault Ground Motions", *SMIP98 Seminar on Utilization of Strong-Motion Data*, Oakland, CA.